The EMBO Journal (2009) 28, 736–744 | © 2009 European Molecular Biology Organization | All Rights Reserved 0261-4189/09
www.embojournal.org

THE EMBO JOURNAL

Erythromycin resistance by L4/L22 mutations and resistance masking by drug efflux pump deficiency

Martin Lovmar[1,3], Karin Nilsson[1], Eliisa Lukk[2], Vladimir Vimberg[2], Tanel Tenson[2] and Måns Ehrenberg[1,*]

[1]Department of Cell and Molecular Biology, Molecular Biology Program, Uppsala University, Uppsala, Sweden and [2]Institute of Technology, University of Tartu, Tartu, Estonia

We characterized the effects of classical erythromycin resistance mutations in ribosomal proteins L4 and L22 of the large ribosomal subunit on the kinetics of erythromycin binding. Our data are consistent with a mechanism in which the macrolide erythromycin enters and exits the ribosome through the nascent peptide exit tunnel, and suggest that these mutations both impair passive transport through the tunnel and distort the erythromycin-binding site. The growth-inhibitory action of erythromycin was characterized for bacterial populations with wild-type and L22-mutated ribosomes in drug efflux pump deficient and proficient backgrounds. The L22 mutation conferred reduced erythromycin susceptibility in the drug efflux pump proficient, but not deficient, background. This 'masking' of drug resistance by pump deficiency was reproduced by modelling with input data from our biochemical experiments. We discuss the general principles behind the phenomenon of drug resistance 'masking', and highlight its potential importance for slowing down the evolution of drug resistance among pathogens.

The EMBO Journal (2009) **28,** 736–744. doi:10.1038/emboj.2009.17; Published online 5 February 2009
Subject Categories: microbiology & pathogens; genomic & computational biology
Keywords: efflux pump; erythromycin; masking; mutation; resistance; ribosome

Introduction

The increasing antibiotic resistance among pathogens creates severe problems in the clinical treatments of bacterial disease. Drug resistance may arise due to the effects of essentially three different mechanisms: modifications of drug target sites, chemical modifications of drugs and increased drug efflux from the bacterial cells. Here, we used *Escherichia coli* strains to study the combined effects of drug efflux efficiency and target mutations on growth inhibition by the ribosome-binding macrolide antibiotic erythromycin. Our findings shed light on the mechanism of erythromycin binding to the ribosome and show 'masking' of target resistance mutations, that is, in a drug efflux pump deficient background, the drug susceptibility is identical for wild-type and target-mutated strains at all external drug concentrations.

Macrolides constitute a growing set of clinically useful antibiotics (Omura, 2002), with the first generation member erythromycin in extensive clinical use for >50 years. The structural mode of erythromycin binding to the entrance of the peptide exit tunnel of the large (50S) ribosomal subunit (Figure 1A) has been characterized at atomic resolution with X-ray crystallography (Schlunzen *et al*, 2001; Tu *et al*, 2005). Although erythromycin and other macrolides bind in the vicinity of the peptidyl-transferase centre (PTC), they do not inhibit peptide bond formation *per se*, but block entrance of the nascent chain to the peptide exit tunnel. This allows for the synthesis of short nascent peptides also in the presence of macrolides, where the maximal peptide length is defined by the space available for peptide growth between the macrolide and the PTC (Tenson *et al*, 2003). In the case of erythromycin, ribosome stalling occurs for nascent peptide lengths between six and eight amino acids (Tenson *et al*, 2003). The stalled ribosome complex may be resolved by peptidyl-tRNA drop-off (Lovmar *et al*, 2004) and recycling of the ribosome to a new round of initiation (Karimi *et al*, 1999). Alternatively, dissociation of erythromycin precedes drop-off, leading to rapid resumption of protein synthesis, now with the ribosome refractory to drug re-binding until the termination and release of the full-length protein (Tenson *et al*, 2003; Lovmar *et al*, 2004). These biochemical data are in line with earlier *E. coli* cell-growth observations, showing erythromycin to inhibit peptide elongation only at or just after initiation of protein synthesis (Andersson and Kurland, 1987).

Mutations in ribosomal RNA and ribosomal proteins conferring reduced macrolide susceptibility (Weisblum, 1995; Vester and Douthwaite, 2001; Zaman *et al*, 2007) were first identified for proteins L4 and L22 in the 50S subunit of the *E. coli* ribosome (Apirion, 1967; Wittmann *et al*, 1973). These mutations, eventually recognized as a lysine to glutamic acid substitution at position 63 of L4 and deletion of methionine, lysine and arginine at positions 82–84 of L22 (Figure 1B) (Chittum and Champney, 1994), will here be referred to as L4(Lys63Glu) and L22(Δ82–84), respectively. Although the equilibrium-binding affinity of erythromycin to the L4 protein seemed greatly reduced by the mutation, the erythromycin affinity to the L22 mutant appeared unaltered by the three amino acids deletion (Wittmann *et al*, 1973). From these qualitative observations, it was suggested that the drug resistance conferred by the L4 mutation is due to strongly reduced binding affinity, but the resistance conferred by the L22 mutation could not be explained. We have now quantified the kinetic effects of the classical L4 and L22 mutations with the help of our cell-free system for protein synthesis with *in vivo* like properties (Pavlov and Ehrenberg, 1996; Lovmar *et al*, 2004). Our data account for the reduced

*Corresponding author. Department of Cell and Molecular Biology, Molecular Biology Program, Uppsala University, Biomedical Centre, Box 596, Husargatan 3, Uppsala 75124, Sweden. Tel.: +46 18 471 42 13; Fax: +49 18 471 42 62; E-mail: ehrenberg@xray.bmc.uu.se
[3]Present address: CMB/Microbiology, University of Gothenburg, Göteborg 40530, Sweden

Received: 6 November 2008; accepted: 8 January 2009; published online: 5 February 2009

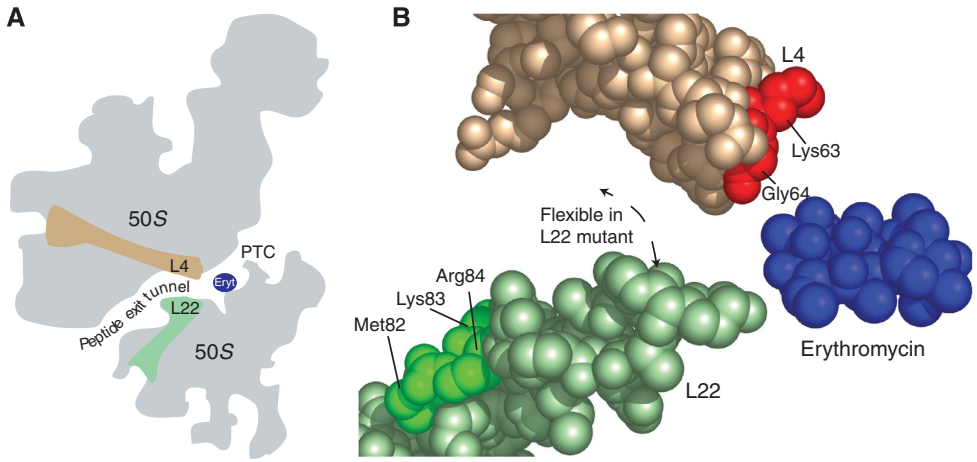

Figure 1 Localization of the erythromycin resistance mutations. (**A**) A cartoon showing a cross-section of the large ribosomal subunit along the nascent peptide exit tunnel, with the peptidyl-transferase centre (PTC) and the subunit interface to the right. The position of the ribosomal proteins L4 and L22 are shown in light brown and green, respectively, and the erythromycin-binding site is indicated in blue. (**B**) The positions of the mutated amino acids in L4 and L22 that leads to erythromycin resistance in relation to the erythromycin-binding site. A dashed arrow indicates the flexibility of the β hairpin in the L22(Δ82–84) mutant (Tu *et al*, 2005). The figure is constructed using the ribosomal proteins from the crystal structure of 70S from *E. coli* (pdb: 2I2V) (Berk *et al*, 2006) combined with erythromycin from (pdb: 1YI2) (Tu *et al*, 2005) by aligning the nucleotide A2058 (*E. coli* numbering) from both structures.

erythromycin susceptibility conferred not only by the L4 but also by the L22 mutations and are compatible with erythromycin entering and exiting the large ribosomal subunit through the nascent peptide exit tunnel (Nissen *et al*, 2000).

To examine whether the relatively small reduction in erythromycin susceptibility by the L22(Δ82–84) mutation could account for its resistance phenotype, we constructed a mathematical model for bacterial growth in the presence of erythromycin with our biochemical data as input. The model predictions were then compared with experimental observations of growing bacterial cultures. The first version of the model (Lovmar *et al*, 2006) did not account for the effects of drug efflux pumps and the resistance phenotype, which motivated the present updated model and the study of the effects of drug efflux pumps on the resistance conferred by the L22(Δ82–84) alteration. Accordingly, we studied the growth-inhibitory action of erythromycin for wild-type and L22-mutated *E. coli* cells in the context of drug efflux proficiency or deficiency; the latter caused by *acrAB–tolC* deletions (Lomovskaya *et al*, 2007). Interestingly, the L22(Δ82–84) mutation conferred strong reduction of erythromycin susceptibility in relation to wild type in the *acrAB–tolC* proficient, intermediate reduction in the *acrB* deficient and no reduction of erythromycin susceptibility in the *tolC* deficient strain, as predicted by the updated model. The reason for this 'resistance masking' by drug efflux pump deficiency is explained in Discussion. Our analysis suggests resistance masking to be a wide-spread phenomenon of potential clinical interest, as it may help to define drug therapeutic schemes that minimize the rate of emergence of target resistance mutations among pathogens.

Results

Kinetics of erythromycin binding to wild-type and mutant ribosomes

To study the mechanisms of erythromycin resistance conferred by the ribosomal protein mutations L22(Δ82–84) and L4(Lys63Glu) (Apirion, 1967; Wittmann *et al*, 1973; Chittum and Champney, 1994), these alterations were engineered into the *E. coli* MG1655 strain. By sequencing, we also identified L4(Δ63–64) as a previously unknown, spontaneously occurring, erythromycin-resistant mutant. In the absence of erythromycin, in a rich LB medium at 37°C, the L22(Δ82–84), L4(Lys63Glu) and L4(Δ63–64) strains had doubling times between 42 and 50 min (corresponding to growth rates μ between 2.8×10^{-4} and $2.3 \times 10^{-4}\,s^{-1}$), whereas the isogenic wild-type MG1655 strain had a doubling time of 29 min (i.e., $\mu = 4.0 \times 10^{-4}\,s^{-1}$). We prepared ribosomes at high activity and purity from these four strains to study the kinetics of their binding to ^{14}C-labelled erythromycin with nitrocellulose (NC) filtration, and all results are summarized in Table I.

Rate constants for erythromycin dissociation from wild-type and mutant ribosomes. Rate constants for dissociation (k_d) of erythromycin from wild-type and mutant ribosomes were obtained from chase experiments. Here, the different ribosome variants were initially equilibrated with ^{14}C-labelled erythromycin, which subsequently was chased with unlabelled erythromycin in excess. The fractions of ribosome-bound ^{14}C-labelled erythromycin remaining at varying incubation times were estimated by NC filtration, and the results are shown in Figure 2. In the wild-type case, the dissociation rate constant was estimated as $0.013\,s^{-1}$, in line with a previous estimate obtained with a different method (Lovmar *et al*, 2004). In the L22 case, the dissociation rate constant was estimated as $0.0011\,s^{-1}$, a value much smaller than the k_d-value in the wild-type case. In the L4 cases, the dissociation rate constants were slightly larger than in the wild-type case, that is, $0.018\,s^{-1}$ for the L4(Lys63Glu) and $0.029\,s^{-1}$ for the L4(Δ63–64) mutant.

Rate constants for erythromycin association to wild-type and L22(Δ82–84) ribosomes. The ribosomes were mixed with ^{14}C-labelled erythromycin at time zero of the incubation and the fractions of erythromycin-bound ribosomes were

Table I Erythromycin-binding properties to wild-type and mutant ribosomes

Strain	k_a ($M^{-1}\,s^{-1}$)	k_d (s^{-1})	K_D (M)
Wt	$(1.0 \pm 0.1) \times 10^6$	$(1.3 \pm 0.06) \times 10^{-2}$	*$(1.2 \pm 0.1) \times 10^{-8}$*
L22 (Δ82–84)	$(1.9 \pm 0.06) \times 10^4$	$(1.1 \pm 0.04) \times 10^{-3}$	*$(5.9 \pm 0.3) \times 10^{-8}$*
L4 (Lys63Glu)	*$(4.0 \pm 0.6) \times 10^3$*	$(1.8 \pm 0.1) \times 10^{-2}$	$(4.6 \pm 0.7) \times 10^{-6}$
L4 (Δ63–64)	*$(9.6 \pm 1) \times 10^3$*	$(2.9 \pm 0.2) \times 10^{-2}$	$(3.0 \pm 0.4) \times 10^{-6}$

Numbers in *italics* are calculated from the other two parameter values for respective strain.

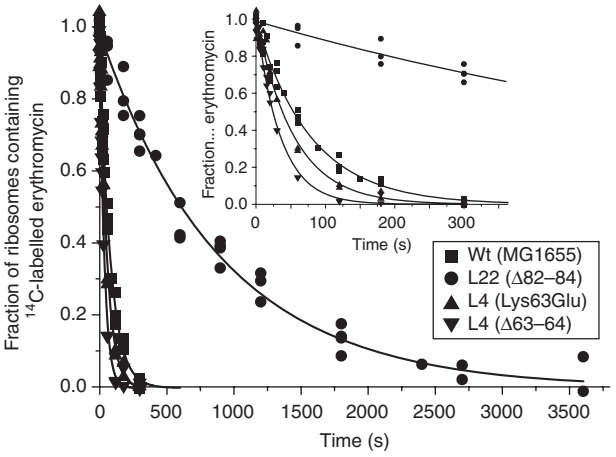

Figure 2 Determination of rate constants for dissociation of erythromycin from wild-type and mutant ribosomes. ^{14}C-labelled erythromycin was pre-bound to wild-type and mutant ribosomes and a chase with a large excess of non-labelled erythromycin started at time zero. At the specified time points, the reactions were quenched with ice-cold buffer and filtered through nitro-cellulose filters. The amount of ^{14}C-labelled erythromycin on the filters corresponds to the amount that remained bound to the ribosomes. The lines are least sum of squares fits to single exponentials and were used to estimate the dissociation rate constants presented in Table I. *Insert*. The same experimental points limited to a short time range between zero and 300 s.

monitored by NC filtering at varying incubation times (Figure 3A and B). The rate constants (k_a) for complex formation between erythromycin and wild-type or L22(Δ82–84) ribosomes were estimated as $1.0\,\mu M^{-1}\,s^{-1}$ (Figure 3A) and $0.019\,\mu M^{-1}\,s^{-1}$ (Figure 3B), respectively. The wild-type k_a estimate is similar to that obtained with a different method (Lovmar *et al*, 2004).

It has been suggested that erythromycin binds to its ribosomal-binding pocket through a pre-equilibrium step (Dinos and Kalpaxis, 2000). We showed earlier that such a putative pre-equilibrium must have an (equilibrium) dissociation constant (K_D) larger than $\sim 1\,\mu M$, that is, much larger than the overall dissociation constant ($\sim 10\,nM$), motivating a one-step approximation for the binding reaction at erythromycin concentrations significantly smaller than 1 μM (Lovmar *et al*, 2004). Here, we show that such a putative pre-equilibrium for the L22(Δ82–84) ribosome must have a K_D-value larger than $\sim 10\,\mu M$ (Figure 3B, insert), motivating a single step approximation for erythromycin binding at erythromycin concentrations significantly smaller than 10 μM.

Equilibrium dissociation constants for complexes between erythromycin and L4(Lys63Glu) or L4(Δ63–64) ribosomes. Because of the low affinity of erythromycin binding to the L4 mutants, it was technically more feasible to estimate the dissociation (equilibrium) (K_D) than the association rate (k_a) constants. The K_D-values for the L4(Lys63Glu) and L4(Δ63–64) mutants were estimated as 4.6 and 3 μM, respectively, from experiments in which the fractions of erythromycin-bound ribosomes were monitored by NC filtration at varying erythromycin concentrations (Figure 4).

Conclusions from the kinetic studies. All three ribosomal mutations reduced the rate constant for erythromycin association by about two orders of magnitude (Table I). This result is compatible with a scenario where erythromycin bind through the nascent peptide exit tunnel with a rate controlled by passage through the L4/L22 constriction, and that this passage was severely obstructed by each one of these mutations (Figure 1A, Discussion). However, also the equilibrium-binding constants were altered by the mutations; corresponding to a 5-, 380- or 250-fold drug affinity reduction by the L22(Δ82–84), L4(Lys63Glu) or L4(Δ63–64) mutations, respectively (Table I). From this, we conclude that the L4/L22 mutations not only obstructed the tunnel passage but *also* modified the erythromycin-binding cleft.

Erythromycin-dependent growth inhibition of wild-type and mutant E. coli populations

We studied the effects of erythromycin on the growth rates of the wild-type and L22(Δ82–84)-mutated variants of the MG1655 *E. coli* strain in a wild-type genetic background or in combination with Δ*tolC* or Δ*acrB* drug efflux pump deficient strains (Okusu *et al*, 1996). The growth rates were estimated as OD-values after 4 h of growth, and the results are shown in Figure 5A and B. In the pump proficient genetic background, the ribosomal wild type was most sensitive to erythromycin, whereas the L22 mutant displayed less drug susceptibility (Figure 5A). The erythromycin sensitivity for the strain with wild-type ribosomes was greatly increased by the Δ*acrB* deletion, but the largest sensitivity was conferred by the Δ*tolC* deletion (Figure 5A). This suggests that the erythromycin efflux pump activity was insignificant for the Δ*tolC* strain, whereas the Δ*acrB* strain retained residual efflux pump activity (see Discussion). The erythromycin susceptibility of the L22 ribosome mutant strain was virtually identical to that of the wild type in the Δ*tolC*, but smaller in the Δ*acrB* genetic background (Figure 5B). Thus, elimination of the drug efflux activity by the Δ*tolC* alteration completely eliminated the growth advantage of the L22 mutation in relation to the strain with wild-type ribosomes.

To investigate whether our kinetic data could quantitatively account for the growth inhibition by erythromycin (Figure 5A and B), we used detailed mathematical modelling, based on these and previous (Lovmar *et al*, 2006) data on ribosome function, to predict the growth rate inhibition

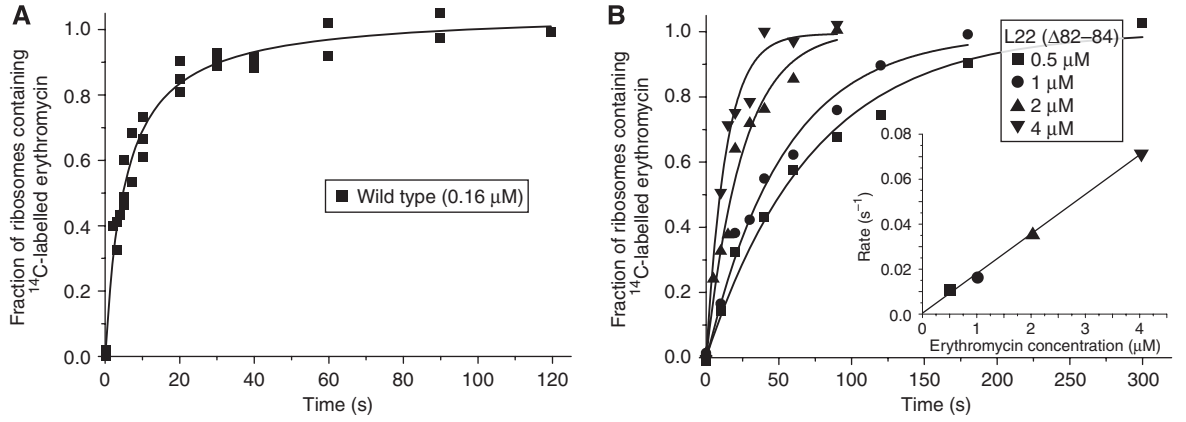

Figure 3 Determination of erythromycin association rate constants for wild-type and L22 mutant ribosomes. The ribosomes were mixed with ^{14}C-labelled erythromycin at time zero, and the reactions at different erythromycin concentrations were quenched with ice-cold buffer containing a large excess of non-labelled erythromycin (to prevent further binding of ^{14}C-labelled erythromycin) at different time points. The quenched reactions were rapidly filtered through nitro-cellulose filters. The line in (**A**) is a least sum of squares fit to a hyperbolic function and the lines in (**B**) are least sum of squares fits to single exponentials. These fits were used to estimate the association rate constants presented in Table I. The insert in (B) shows the rates of erythromycin association to the L22-mutated ribosomes as a function of the erythromycin concentration.

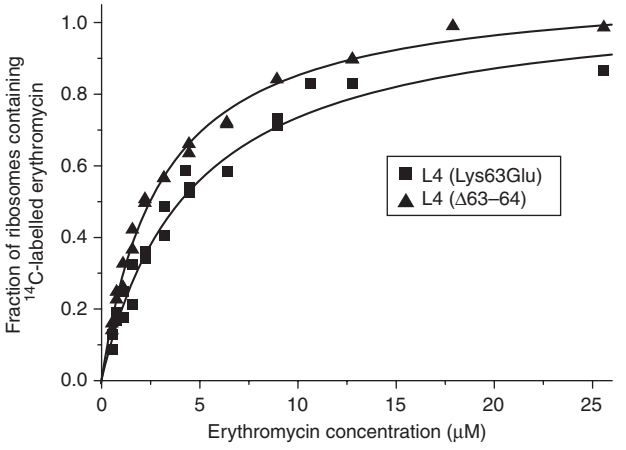

Figure 4 Determination of equilibrium dissociation constants for both L4 mutants. The ribosomes were mixed with different concentrations of ^{14}C-labelled erythromycin and incubated for 15 min before it was quenched with cold buffer and rapidly filtered through nitro-cellulose filters. The lines are least sum of squares fits to a hyperbolic function and were used to estimate the equilibrium dissociation constants presented in Table I.

curves for the wild type and L22-mutated *E. coli* strains as displayed in Figure 5C and D. The model is briefly described in Materials and methods and in full detail in Supplementary data. It reflects the complex mechanism of action of erythromycin (Supplementary data; Lovmar *et al* (2004, 2006)), but neglects erythromycin induction of changes in the transcriptional profile (Goh *et al*, 2002), induction of stress response pathways (VanBogelen and Neidhardt, 1990) and erythromycin-dependent inhibition of the assembly of ribosomal subunits (Champney and Burdine, 1995; Siibak *et al*, 2009). Despite its approximate nature, the model accurately reproduces the growth rate advantage conferred by the L22 mutation in the drug efflux proficient background (compare the two upper curves of Figure 5A with those of Figure 5C) as well as the masking of this growth rate advantage in the Δ*tolC* background (compare the lower curves of Figure 5B with those in Figure 5D). The model also reproduces the experimental finding that strains with wild-type ribosomes have the same drug susceptibility in the Δ*tolC* and Δ*acrB* backgrounds, whereas strains with L22-mutated ribosomes grow faster in the Δ*acrB* than in the Δ*tolC* background (compare Figure 5B with D). These features reflect general principles of target resistance masking, as explained in the Discussion.

Discussion

How does erythromycin interact with the ribosome?

In the first biochemical study of the L22(Δ82–84) and L4(Lys63Glu) resistance mutations, it was proposed from qualitative experiments that erythromycin bound similarly to the L22(Δ82–84) and wild-type ribosomes, whereas the affinity of erythromycin to the L4(Lys63Glu) variant was very weak (Wittmann *et al*, 1973). Our quantitative biochemical data now show that the L4(Lys63Glu) and L22(Δ82–84) ribosomes had equilibrium dissociation constants (K_D) for erythromycin binding about 380- and 5-fold larger than wild-type ribosomes, respectively (Figures 2–4 and Table I). The association rate constants (k_a) for all ribosomal mutants were about two orders of magnitude smaller than the k_a-value for wild-type ribosomes. The rate constants for erythromycin dissociation (k_d) from the L4(Lys63Glu) and L4(Δ63–64) variants were larger than the wild-type k_d-value, whereas the k_d-value of the L22(Δ82–84) mutant was more than 10-fold smaller than the wild-type k_d-value. To interpret these striking kinetic changes caused by the L22 and L4 alterations, we need to know how erythromycin enters and exits its binding pocket on the 50S ribosomal subunit.

Using rolling sphere simulations on crystallographic atom coordinates, Moore and colleagues showed the peptide exit tunnel wall to be impermeable to molecules with the size of erythromycin (Voss *et al*, 2006). Therefore, erythromycin must either bind from the subunit interface through the PTC or through the L4/L22 constriction in the peptide exit tunnel of the 50S subunit (Figure 1A). The similar kinetics of erythromycin binding to initiation complexes (Lovmar *et al*, 2004), empty ribosomes (Table I) and 50S subunits (data not shown) makes binding through the interface less likely, as

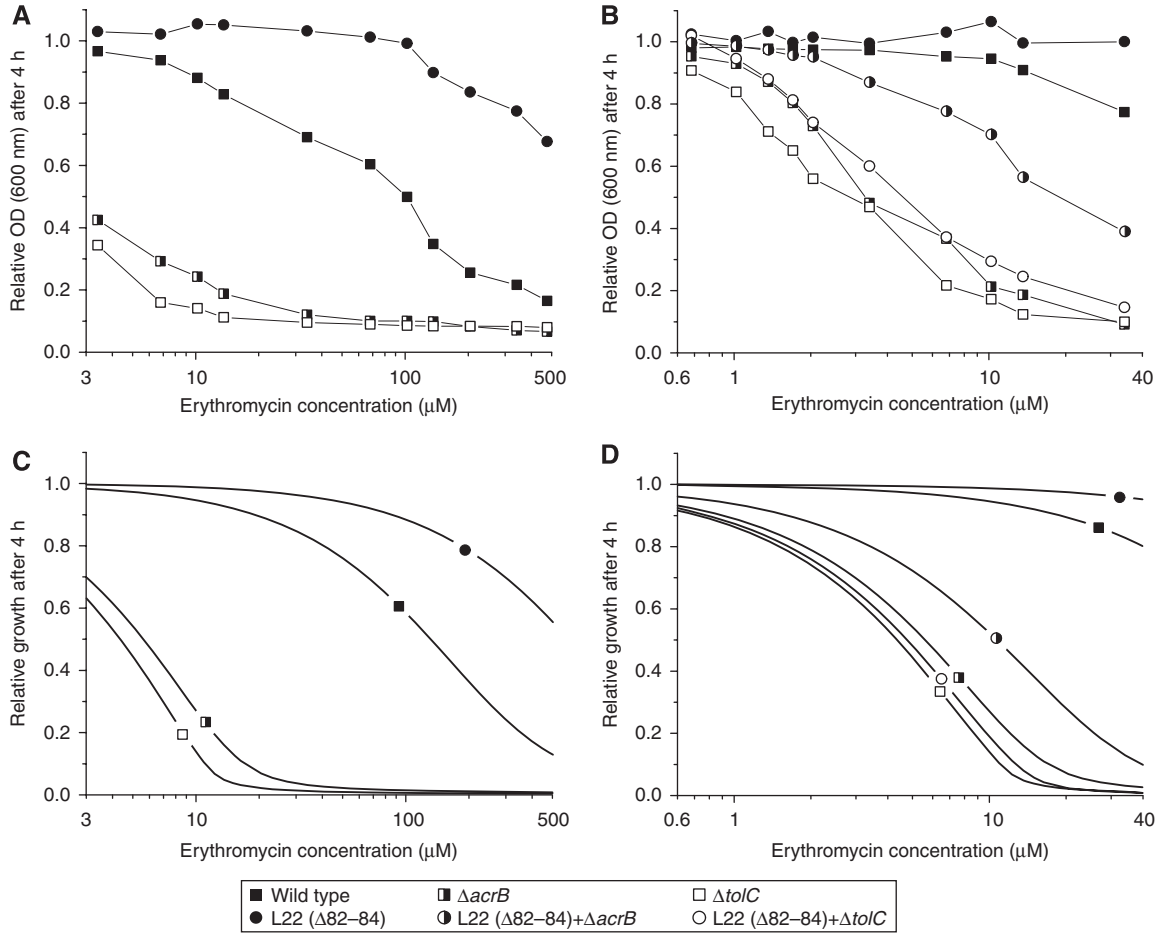

Figure 5 Erythromycin sensitivity measurements. The relative ODs after 4 h are plotted as a function of the erythromycin concentration. The values are normalized to the ODs reached after 4 h in the absence of erythromycin. (**A**) The results of an erythromycin titration in the concentration range required for inhibiting growth in *E. coli* with intact AcrAB–TolC efflux pumps. The level of resistance caused by the ribosomal protein mutants is best shown in this range. (**B**) The results of an erythromycin titration in the lower concentration range required to study the efflux pump mutants. (**C**, **D**) The corresponding simulation using the estimated binding constants (Supplementary data).

entry through the tunnel is expected to be unaffected by 70S ribosome and 70S initiation complex formation, whereas entry through the PTC is expected to vary by subunit docking and P-site filling. If this interpretation is correct, one would also expect mutations in ribosomal proteins L4 and L22, defining the narrowest and rate limiting passage through the peptide exit tunnel (Figure 1), to affect the rate constants for erythromycin's association to (k_a) and dissociation from (k_d) the ribosome. In line with this, our experiments show greatly reduced k_a-values by the L22 and L4 alterations (Table I).

Further information of how erythromycin gains access to its binding pocket has come from cryo-EM reconstructions of the L4(Lys63Glu) and L22(Δ82–84) ribosome variants (Gabashvili *et al*, 2001). It was found that the L4 mutation significantly narrowed the L4/L22-defined constriction in the exit tunnel, in line with the greatly reduced k_a-values resulting from both the L4(Lys63Glu) and the L4(Δ63–64) mutations observed here (Table I). In contrast, the cryo-EM data suggested a widening of the peptide exit tunnel by the L22(Δ82–84) mutation (Gabashvili *et al*, 2001). From this observation and the suggestion that the L22(Δ82–84) mutation did not alter the affinity of erythromycin to the ribosome (Wittmann *et al*, 1973), Gabashvili *et al* proposed that the erythromycin-dependent blockage of the peptide exit tunnel for nascent chain entry was by-passed by tunnel broadening due to the L22(Δ82–84) mutation. Our data show a five-fold reduction in erythromycin affinity to the ribosome and about two orders of magnitude reduction in the association rate constant by the L22(Δ82–84) mutation (Table I). These kinetic changes fully account for the erythromycin resistance conferred by the L22(Δ82–84) alteration, making the nascent chain by-pass model redundant. In addition, during the review process of this paper, a report showing that protein synthesis on L22-mutated ribosomes in a cell lysate can be 100% inhibited by erythromycin was published (Moore and Sauer, 2008). This observation gives direct evidence against the nascent chain by-pass model, which predicts continued protein synthesis also when the ribosomes are saturated with erythromycin, and thus gives support to our resistance mechanism, based on reduced drug affinity by the L22 mutation.

At first sight, the cryo-EM observation of a broadened peptide exit tunnel (Gabashvili *et al*, 2001) appeared incompatible with the slow association kinetics we have observed for the L22(Δ82–84) mutant. However, recent atomic resolution X-ray crystal data on the L22(Δ82–84) ribosome (Tu *et al*, 2005) suggest that the cryo-EM interpretation may be an over simplification. Tu *et al* show that the peptide loop in L22, that

is part of the peptide exit tunnel constriction, becomes bent and more flexible by the L22(Δ82–84) alteration (Figure 1B). Accordingly, it is likely that the apparent broadening of the exit tunnel seen by cryo-EM is caused by a loss of visible density due to the flexibility of the L22 loop. The question is now whether the altered conformation and increased flexibility of the L22(Δ82–84) loop identified by crystallography (Tu *et al*, 2005) can explain the slow kinetics we observed for L22(Δ82–84) mutant (Table I).

The function of the L4/L22 constriction has remained obscure but is likely to include the signaling of nascent peptide sequence motifs to other parts of the ribosome (Tenson and Ehrenberg, 2002). One may, in addition, assume that the L4/L22 constriction has evolved to facilitate rapid transport of the bulk of nascent chains through the tunnel. Therefore, mutations in L4 and L22 are expected to cause suboptimal tunnel passage of nascent chains and, putatively, other ligands like erythromycin. In line with this, we suggest that the increased freedom of movement of the L22 constriction loop by L22(Δ82–84) alteration results in a distribution of conformations that obstruct, rather than facilitate, the transport of erythromycin (Table I) and perhaps other drugs through the tunnel.

Accordingly, we propose that the passage through the tunnel constriction, defined by the L4 and L22 ribosomal proteins, is the rate limiting step for erythromycin binding to its 50S pocket (Figure 1) (Schlunzen *et al*, 2001; Tu *et al*, 2005). We note that if the L4 and L22 mutations had affected tunnel transport only, they would have left the K_D-values unaltered by equal reductions in k_a- and k_d-values, which is not the case (Table I). Therefore, these mutations not only obstruct tunnel constriction passage but also distort the erythromycin-binding pocket, resulting in the 5-, 380- or 250-fold drug affinity reduction by the L22(Δ82–84), L4(Lys63Glu) or L4(Δ63–64) mutations, respectively (Table I).

Masking of target resistance mutations by drug efflux deficiency

Our *in vivo* observations show that, in the presence of erythromycin, the growth advantage conferred by the L22 ribosomal mutation in the drug efflux proficient genetic background (Figure 5A) is reduced in the Δ*acrB* and completely absent in the Δ*tolC* background (Figure 5B). The intermediate scenario for the Δ*acrB* mutant may be explained by alternative drug efflux pumps, for example, MdtEF (previously YhiUV) (Nishino and Yamaguchi, 2001) and MacAB (Kobayashi *et al*, 2001), which recognize erythromycin and require the outer membrane pore TolC to function. The observation that drug efflux deficiency leads to increased drug sensitivity is expected, but why drug efflux deficiency should mask the effects of target resistance mutations is less obvious.

Our bacterial growth modelling (Supplementary data) with biochemical input data reproduces the complete masking of the effect of the L22 resistance mutation observed in the Δ*tolC* and the partial masking of this effect observed in the Δ*acrB* background (compare Figure 5B and D). The model is complex (Supplementary data), due to the complex mechanism of erythromycin action (Lovmar *et al*, 2006), but some of its essential properties are robust and do not depend on the mechanistic details of growth inhibition by antibiotic drugs.

We note, firstly, that the intracellular free and target-bound drug concentrations were equilibrated under our experimental conditions. The steady-state condition for equilibration is in general that the growth rate, μ, is much smaller than the rate constant, k_d, for drug dissociation from the target (Fange *et al*, submitted). This follows, as the intracellular equilibration rate is set by the k_d-value and the shift from equilibrium is determined by the μ-value, so that exact equilibration is established when $\mu = 0$. To prove our point, it is sufficient to inspect the L22 mutant, which had the by far smallest k_d-value of $1.1 \times 10^{-3}\,s^{-1}$ (Table I). As the μ-value for that mutant was equal to $2.6 \times 10^{-4}\,s^{-1}$ (i.e., 45 min doubling time) without drug addition and successively smaller in the presence of increasing concentrations of erythromycin in the medium, μ was always much smaller than k_d.

Secondly, the masking phenomenon depends, in fact, only on the pathway by which drug influx is balanced during steady state growth in drug-containing media (Fange *et al*, submitted). To see this, we note that there are essentially three pathways by which the concentration of drug molecules in the cytoplasm of bacteria is reduced. The first is transport out from the cell by passive diffusion or by the action of efflux pumps. The second is degradation or modification of drugs by endogenous enzymes of the pathogen. The third is drug dilution by cell growth and division (dilution-by-growth). The efficiency of the first two pathways depends on the free-intracellular concentration of the drug, whereas the third pathway affects free and target-bound drug alike. When the targets are 'strong' in the sense that they have high concentration and high affinity to the drug and the efflux pumps (and/or drug-degrading enzymes) are comparatively 'weak', the-dilution by-growth pathway for drug reduction dominates, in which case the total (free plus target bound) drug concentrations in wild-type and mutant cells are similar. The erythromycin-binding wild-type and L22(Δ82–84) altered ribosomes are both strong targets due to high intracellular concentration (in micromolar range) and high affinity to the drug ($K_D = 12$ and 59 nM, respectively). In the absence of efficient efflux pumps, the total intracellular drug concentrations are equal due to third pathway dominance. Thus, the fractions of drug-bound ribosomes and growth rates of wild-type and L22(Δ82–84) mutant will be virtually identical (Figure 5B and D). When, in contrast, the pump (and/or drug-degradation) efficiency is very high, like in the presence of AcrAB–TolC, then the two first pathways for drug concentration decrease dominate. In all cases where the first two pathways dominate, the growth-inhibitory action of antibiotics correlates positively with the target affinity to the drug. That is, in those cases target resistance mutations will be expressed as reduced drug susceptibility and increased MIC-values of the pathogens (Figure 5A and C).

Interestingly, target resistance masking by drug efflux deficiency is not idiosyncratic for *E. coli* or erythromycin. It has been observed for different organisms, drugs and drug targets (e.g., Peric *et al*, 2003; Cagliero *et al*, 2005, 2006). These studies show that MIC-values, greatly varying between target site mutants or between mutants and wild type in a drug efflux pump proficient background, converge to one and the same (and evidently much smaller) MIC-value in a drug efflux pump deficient background, that is, the target binding differences become 'masked' by efflux pump inhibition. From the striking similarity between our data (Figure 5), showing

converging MIC-values of erythromycin for wild-type and L22 mutant ribosomes in the Δ*tolC* background, and these previous observations, we suggest that the mechanism for resistance masking outlined here accounts for all these experimental observations.

During the review process of this work, a report on the growth-inhibitory action of erythromycin on wild-type and L22(Δ82–84) ribosomes in drug efflux pump proficient and deficient backgrounds was published (Moore and Sauer, 2008). Their results confirmed the existence of drug target resistance masking by drug efflux pump deficiency, as seen here (Figure 5), but they missed that the L22(Δ82–84) mutation decreases the affinity of erythromycin to the ribosome. To explain erythromycin resistance only in the drug efflux pump proficient background, they instead made the *ad hoc* suggestion that the L22(Δ82–84) mutation enhanced drug efflux pump efficiency by modifying ribosomal stalling properties (Moore and Sauer, 2008).

Pump efflux deficiency and the rate of evolution of drug resistance among pathogens

It is frequently observed that efflux pump deficiency greatly slows down the evolution of resistance among bacterial pathogens against various antibiotic drugs (e.g., Lomovskaya *et al*, 1999, 2001; Markham, 1999; Ricci *et al*, 2006). These findings highlight the importance of developing highly efficient efflux pump inhibitors to slow down the emergence of antibiotic resistance among pathogens (Lomovskaya *et al*, 2001). The obvious reason for why efflux pump deficiency prevents drug resistance is that it greatly increases the susceptibility of, in particular, gram-negative bacterial pathogens to antibiotic drugs. However, as explained in the previous section and described in full mathematical detail in (Fange *et al*, submitted), there is yet another and previously unexplored mechanism by which pump deficiency can slow down the evolution of drug resistance. That is, for 'strong' targets drug efflux deficiency leads to uniform MIC-values for all target mutations that preserve bacterial growth as the dominant pathway for reducing the intracellular drug concentration, as observed in Figure 5B. This means that for any drug concentration, all the way up to the MIC-value such target mutations will confer no selective advantage compared with the wild-type target. As, at the same time, there must be a selective advantage for a mutant to become dominant in the population, the 'masking' of the benefit of target resistance by pump efflux deficiency may effectively prevent the spread of mutants with reduced drug susceptibility. We are presently studying these intriguing scenarios of potential clinical relevance with biochemical and population genetic approaches.

Materials and methods

Chemicals and buffers

GTP and ATP were from GE Healthcare. Putrescine, spermidine, phosphoenolpyruvate (PEP) and erythromycin were from Sigma-Aldrich. [^{14}C]erythromycin was from Perkin-Elmer. Pyruvate kinase was from Boehringer-Mannheim. NC filters Protran BA85 were from VWR.

All cell-free experiments were performed at 37°C in polymix buffer (Jelenc and Kurland, 1979; Antoun *et al*, 2004) supplemented with 1 mM GTP, 1 mM ATP and 10 mM PEP.

Procedures

Construction of mutations in ribosomal protein L4 and L22 in an isogenic background. E. coli MG1655 cells (Blattner *et al*, 1997), transformed with plasmid pKD46 (Datsenko and Wanner, 2000) were grown in SOB medium containing ampicillin (100 μg/ml). A measure of 20 ml of the culture was grown at 30°C until OD(A600 nm) 0.6. The cells were collected by centrifugation (8 min, 5500 *g*, 4°C) and resuspended in ice-cold sterile water. The washing procedure was repeated two more times, and the cells were finally resuspended in 100 μl of water. About 50 μl of the cells were electroporated with 10 ng (3 μl) of DNA oligonucleotide using Bio-Rad Gene Pulser at 1.8 kV, 25 μF (2 mm cuvettes). The electroporated cells were diluted with 1 ml of LB medium, incubated for 2 h at 37°C and plated on LB-agar containing erythromycin (300 μg/ml). The recombinase coding plasmid pKD46 was removed as described previously (Datsenko and Wanner, 2000). The mutations were confirmed by sequencing. The L4(Δ63–64) mutant appeared spontaneously and was discovered during construction of the L4(Lys63Glu) mutant.

Oligonucleotides used:

L4(Lys63Glu) TAACTGGTTCCGGTAAAAAACCG_TGGCGCCAGGA AGGCACCGGC_CGTGCGCGTTCTGGTTCTATCAAGAG

L22(Δ82–84) AAGTTACGAAAATTTTCGTAGACGAAGGC_CCGAGC ATTATG_CCGCGTGCAAAAGGTCGTGCAGATCGCAT

Construction of the double mutants. The *acrB* and *tolC* knockouts were made in both the wild-type and the erythromycin-resistant strains (described above) by using the method of Datsenko and Wanner (2000). The PCR products for transforming the strains were made from plasmid pKD13 with following oligonucleotides:

TolC1(/forward)/: AATTTTACAGTTTGATCGCGCTAAATACTGCT TCACAAGGAATGCAAGTGTAGGCTGGAGCT GCTTC

TolC2(/reverse)/: TTTACGTTGCCTTACGTTCAGACGGGGCCGA AGCCCCGTCGTCATCAATTCCGGGGATCCGTC GACC

AcrB1(/forward)/: TGCTCAGCCTGAACAGTCCAAGTCTTAACTTA AACAGGAGCCGTTAAGACGTGTAGGCTGGAG CTGCTTC

AcrB2(/reverse)/: ATGCATAAAAAAGGCCGCTTACGCGGCCTTA GTGATTACACGTTGTATCAATTCCGGGGATCC GTCGACC

Inhibition curves. Overnight cultures were diluted into 10 ml of LB medium to OD (600 nm) 0.1. The cultures were grown at 37°C until OD 0.4–0.6 and again diluted to OD 0.1. A measure of 2 ml of the culture was used for one experimental point; erythromycin was added at concentrations indicated. OD was measured after 4 h of growth at 37°C. In control experiments in the absence of erythromycin all strains grew exponentially during the 4-h incubation time.

Ribosome purification. Mutant and wild-type ribosomes were purified by ultra-centrifugation as described previously (Tenson *et al*, 2003). Bacterial DNA from aliquots of the cultures used for purification was used for sequencing of the L4 and L22 coding genes to ensure the absence of revertants among the purified ribosomes.

Nitrocellulose filter assays. Ribosomes stick to NC filters whereas erythromycin does not. Hence, the NC filter assay allows us to separate ribosome-bound [^{14}C]erythromycin from the free [^{14}C]erythromycin. The filters were pre-soaked in cold polymix buffer containing 10 μM erythromycin. After each sample was applied, the filter was rapidly washed twice with 1 ml ice-cold polymix buffer before the radioactivity on the filter was measured in a scintillation counter.

Chase experiment. The ribosome mixture contained ~2 μM ribosomes (wild type or mutant) and [^{14}C]erythromycin (10 μM), and the chase mixture contained 225 μM erythromycin. After mixing 20 μl of the ribosome mixture with 20 μl of the chase mixture, reactions were quenched at different times by addition of 1 ml ice-cold polymix and then rapidly applied to the NC filter.

Least square fitting of these data points (i.e., bound fraction versus time) to a single exponential function gives the erythromycin

dissociation rate constants from wild-type and mutant ribosomes as presented in Table I.

Association rate experiment. The ribosome mixture contained ~0.32 μM wild-type ribosomes or ~0.2 μM L22-mutant ribosomes, and the erythromycin mixture contained [^{14}C]erythromycin (at different concentrations). After mixing 40 μl of the ribosome mixture with 40 μl of the erythromycin mixture, reactions were quenched at different times by addition of 1 ml ice-cold polymix containing 40 μM erythromycin and then rapidly applied to the NC filter.

Least square fitting of the data points (i.e., bound fraction versus time) to a hyperbolic function gives the erythromycin association rate constant to the wild-type ribosomes (Table I) because the concentration of erythromycin is similar to the concentration of ribosomes in the experiment. In contrast, the data points for the L22 mutant were fitted to single exponential functions because the concentration of erythromycin in this setup was much higher than the ribosome concentration. Thus, the free-erythromycin concentration can be regarded as a constant throughout the experiment. The linear relation between the estimated rates and the erythromycin concentration was used to estimate the erythromycin association rate constant for the L22-mutant ribosome presented in Table I.

Equilibrium-binding experiment. The ribosome mixture contained ~0.7 μM L4-mutant ribosomes, and the erythromycin mixture contained [^{14}C]erythromycin (at different concentrations). After mixing 40 μl of the ribosome mixture with 40 μl of the erythromycin mixture, reactions were incubated for ~15 min before it was quenched with 1 ml ice-cold polymix buffer and then rapidly applied to the NC filter.

Least sum of squares fitting of these data points (i.e., bound fraction versus erythromycin concentration) to a hyperbolic function gives the erythromycin equilibrium-binding constants for both L4 mutants as presented in Table I.

Cell-growth simulations. On the basis of our previously published model for peptide-mediated erythromycin resistance (Lovmar *et al*, 2006), we set up a system of differential equations of the large ribosomal subunit in different states in a growing system, that is, each equation contains a term for dilution. The model accounts for changes in the total concentration of intracellular erythromycin by the passive inflow and outflow of erythromycin over the cell membranes and the active transport out from the cell by the AcrAB–TolC pump system. The system of equations was solved numerically by Euler's method, after the introduction of a certain erythromycin concentration in the growth medium. To compare the simulations with the turbidity of cells in the cell-growth experiments, we registered the simulated volume expansion during the first 4 h after addition of erythromycin. The change in volume of the simulated system corresponds to the change in the sum of the cytoplasmic volumes, and it is therefore proportional to the change in OD of the culture. Before erythromycin exposure, the system resided at steady state. The used program software was MATLAB 6.5 (The MathWorks Inc., Natick, MA). A detailed description of the model and the parameter values used are presented in the on-line Supplementary data.

Supplementary data

Supplementary data are available at *The EMBO Journal* Online (http://www.embojournal.org).

Acknowledgements

We thank Drs Richard Buckingham and Carl-Henrik Heldin, for valuable discussions, and Drs Stephen Douthwaite and Marko Kervinen for valuable comments on the manuscript. This work was supported by grants from the Swedish Research Council (ML and ME), NIH (GM70768) (ME), the Wellcome Trust International Senior Fellowship (070210/Z/03/Z) (TT) and the Estonian Science Foundation grant no. 6768 (TT).

References

Andersson S, Kurland CG (1987) Elongating ribosomes *in vivo* are refractory to erythromycin. *Biochimie* **69:** 901–904

Antoun A, Pavlov MY, Tenson T, Ehrenberg MM (2004) Ribosome formation from subunits studied by stopped-flow and Rayleigh light scattering. *Biol Proced Online* **6:** 35–54

Apirion D (1967) Three genes that affect Escherichia coli ribosomes. *J Mol Biol* **30:** 255–275

Berk V, Zhang W, Pai RD, Cate JH (2006) Structural basis for mRNA and tRNA positioning on the ribosome. *Proc Natl Acad Sci USA* **103:** 15830–15834

Blattner FR, Plunkett III G, Bloch CA, Perna NT, Burland V, Riley M, Collado-Vides J, Glasner JD, Rode CK, Mayhew GF, Gregor J, Davis NW, Kirkpatrick HA, Goeden MA, Rose DJ, Mau B, Shao Y (1997) The complete genome sequence of Escherichia coli K-12. *Science* **277:** 1453–1474

Cagliero C, Mouline C, Cloeckaert A, Payot S (2006) Synergy between efflux pump CmeABC and modifications in ribosomal proteins L4 and L22 in conferring macrolide resistance in Campylobacter jejuni and Campylobacter coli. *Antimicrob Agents Chemother* **50:** 3893–3896

Cagliero C, Mouline C, Payot S, Cloeckaert A (2005) Involvement of the CmeABC efflux pump in the macrolide resistance of Campylobacter coli. *J Antimicrob Chemother* **56:** 948–950

Champney WS, Burdine R (1995) Macrolide antibiotics inhibit 50S ribosomal subunit assembly in Bacillus subtilis and Staphylococcus aureus. *Antimicrob Agents Chemother* **39:** 2141–2144

Chittum HS, Champney WS (1994) Ribosomal protein gene sequence changes in erythromycin-resistant mutants of Escherichia coli. *J Bacteriol* **176:** 6192–6198

Datsenko KA, Wanner BL (2000) One-step inactivation of chromosomal genes in Escherichia coli K-12 using PCR products. *Proc Natl Acad Sci USA* **97:** 6640–6645

Dinos GP, Kalpaxis DL (2000) Kinetic studies on the interaction between a ribosomal complex active in peptide bond formation and the macrolide antibiotics tylosin and erythromycin. *Biochemistry* **39:** 11621–11628

Gabashvili IS, Gregory ST, Valle M, Grassucci R, Worbs M, Wahl MC, Dahlberg AE, Frank J (2001) The polypeptide tunnel system in the ribosome and its gating in erythromycin resistance mutants of L4 and L22. *Mol Cell* **8:** 181–188

Goh EB, Yim G, Tsui W, McClure J, Surette MG, Davies J (2002) Transcriptional modulation of bacterial gene expression by subinhibitory concentrations of antibiotics. *Proc Natl Acad Sci USA* **99:** 17025–17030

Jelenc PC, Kurland CG (1979) Nucleoside triphosphate regeneration decreases the frequency of translation errors. *Proc Natl Acad Sci USA* **76:** 3174–3178

Karimi R, Pavlov MY, Buckingham RH, Ehrenberg M (1999) Novel roles for classical factors at the interface between translation termination and initiation. *Mol Cell* **3:** 601–609

Kobayashi N, Nishino K, Yamaguchi A (2001) Novel macrolide-specific ABC-type efflux transporter in Escherichia coli. *J Bacteriol* **183:** 5639–5644

Lomovskaya O, Lee A, Hoshino K, Ishida H, Mistry A, Warren MS, Boyer E, Chamberland S, Lee VJ (1999) Use of a genetic approach to evaluate the consequences of inhibition of efflux pumps in Pseudomonas aeruginosa. *Antimicrob Agents Chemother* **43:** 1340–1346

Lomovskaya O, Warren MS, Lee A, Galazzo J, Fronko R, Lee M, Blais J, Cho D, Chamberland S, Renau T, Leger R, Hecker S, Watkins W, Hoshino K, Ishida H, Lee VJ (2001) Identification and characterization of inhibitors of multidrug resistance efflux pumps in Pseudomonas aeruginosa: novel agents for combination therapy. *Antimicrob Agents Chemother* **45:** 105–116

Lomovskaya O, Zgurskaya HI, Totrov M, Watkins WJ (2007) Waltzing transporters and 'the dance macabre' between humans and bacteria. *Nat Rev Drug Discov* **6:** 56–65

Lovmar M, Nilsson K, Vimberg V, Tenson T, Nervall M, Ehrenberg M (2006) The Molecular mechanism of peptide-mediated erythromycin resistance. *J Biol Chem* **281:** 6742–6750

Lovmar M, Tenson T, Ehrenberg M (2004) Kinetics of macrolide action: the josamycin and erythromycin cases. *J Biol Chem* **279:** 53506–53515

Markham PN (1999) Inhibition of the emergence of ciprofloxacin resistance in Streptococcus pneumoniae by the multidrug efflux inhibitor reserpine. *Antimicrob Agents Chemother* **43:** 988–989

Moore SD, Sauer RT (2008) Revisiting the mechanism of macrolide-antibiotic resistance mediated by ribosomal protein L22. *Proc Natl Acad Sci USA* **105:** 18261–18266

Nishino K, Yamaguchi A (2001) Analysis of a complete library of putative drug transporter genes in Escherichia coli. *J Bacteriol* **183:** 5803–5812

Nissen P, Hansen J, Ban N, Moore PB, Steitz TA (2000) The structural basis of ribosome activity in peptide bond synthesis. *Science* **289:** 920–930

Okusu H, Ma D, Nikaido H (1996) AcrAB efflux pump plays a major role in the antibiotic resistance phenotype of Escherichia coli multiple-antibiotic-resistance (Mar) mutants. *J Bacteriol* **178:** 306–308

Omura S (2002) *Macrolide Antibiotics: Chemistry, Biology, and Practice*. Orlando: Academic Press

Pavlov MY, Ehrenberg M (1996) Rate of translation of natural mRNAs in an optimized *in vitro* system. *Arch Biochem Biophys* **328:** 9–16

Peric M, Bozdogan B, Jacobs MR, Appelbaum PC (2003) Effects of an efflux mechanism and ribosomal mutations on macrolide susceptibility of Haemophilus influenzae clinical isolates. *Antimicrob Agents Chemother* **47:** 1017–1022

Ricci V, Tzakas P, Buckley A, Piddock LJ (2006) Ciprofloxacin-resistant Salmonella enterica serovar Typhimurium strains are difficult to select in the absence of AcrB and TolC. *Antimicrob Agents Chemother* **50:** 38–42

Schlunzen F, Zarivach R, Harms J, Bashan A, Tocilj A, Albrecht R, Yonath A, Franceschi F (2001) Structural basis for the interaction of antibiotics with the peptidyl transferase centre in eubacteria. *Nature* **413:** 814–821

Siibak T, Peil L, Xiong L, Mankin A, Remme J, Tenson T (2009) Erythromycin- and chloramphenicol-induced ribosomal assembly defects are secondary effects of protein synthesis inhibition. *Antimicrob Agents Chemother* **53:** 563–571

Tenson T, Ehrenberg M (2002) Regulatory nascent peptides in the ribosomal tunnel. *Cell* **108:** 591–594

Tenson T, Lovmar M, Ehrenberg M (2003) The mechanism of action of macrolides, lincosamides and streptogramin B reveals the nascent Peptide exit path in the ribosome. *J Mol Biol* **330:** 1005–1014

Tu D, Blaha G, Moore PB, Steitz TA (2005) Structures of MLS(B)K antibiotics bound to mutated large ribosomal subunits provide a structural explanation for resistance. *Cell* **121:** 257–270

VanBogelen RA, Neidhardt FC (1990) Ribosomes as sensors of heat and cold shock in Escherichia coli. *Proc Natl Acad Sci USA* **87:** 5589–5593

Vester B, Douthwaite S (2001) Macrolide resistance conferred by base substitutions in 23S rRNA. *Antimicrob Agents Chemother* **45:** 1–12

Voss NR, Gerstein M, Steitz TA, Moore PB (2006) The geometry of the ribosomal polypeptide exit tunnel. *J Mol Biol* **360:** 893–906

Weisblum B (1995) Erythromycin resistance by ribosome modification. *Antimicrob Agents Chemother* **39:** 577–585

Wittmann HG, Stoffler G, Apirion D, Rosen L, Tanaka K, Tamaki M, Takata R, Dekio S, Otaka E (1973) Biochemical and genetic studies on two different types of erythromycin resistant mutants of Escherichia coli with altered ribosomal proteins. *Mol Gen Genet* **127:** 175–189

Zaman S, Fitzpatrick M, Lindahl L, Zengel J (2007) Novel mutations in ribosomal proteins L4 and L22 that confer erythromycin resistance in Escherichia coli. *Mol Microbiol* **66:** 1039–1050

